Dynamic models of earthquakes in the Eastern San Gorgonio Pass

Report for SCEC Award #16229
Submitted June 6, 2017

Investigators: David D. Oglesby (UC Riverside), Michele L. Cooke (UMass Amherst)

A. Background

One of the most important seismological issues in Southern California is the maximum probable earthquake size along the San Andreas fault (SAF). Resolving this issue may hinge on understanding the rupture behavior in the San Gorgonio Pass (SGP): in this region, the San Andreas fault system forms a restraining bend that may serve as a "pinch point" for ruptures along the fault system. While portions of the SAF to the north and south of the San Gorgonio Pass (SGP) have single active strands that are continuous, in the SGP the SAF follows what appear to be several non-vertical and non-coplanar active segments [e.g., *Yule*, 2009] (Figure 1). Paleoseismic data suggest that the SGP may be a barrier to many but not all earthquakes that propagate from south or north along the SAF [*Heermance et al.*, 2015]. The behavior of rupture through the SGP is of fundamental importance to the maximum earthquake size in Southern California, the rate of large to great earthquakes, ground motion, and seismic hazard. In particular, simulations have shown that Northwesterly-directed rupture on the SAF may channel seismic radiation directly toward the Los Angeles Basin, where radiation is amplified by basin sediments leading to very high and long duration ground motion [*Olsen et al.*, 2008]. Thus, the issue of whether the San Gorgonio Pass serves as a significant barrier to earthquake rupture propagation is of great practical as well as theoretical interest.

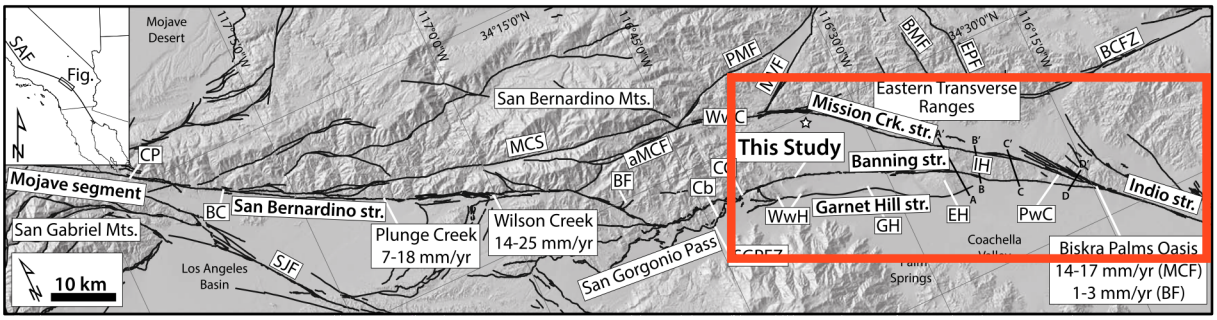

Figure 1. Fault map of San Gorgonio Pass. Our area of dynamic modeling is outlined in Red. Modified from Gold et al. [2015].

Of particular interest is the behavior of earthquake ruptures that approach the Eastern edge of the San Gorgonio Pass. In this region, the Coachella segment of the SAF splits into the Mission Creek and Banning strands (Fig 1). West of this branch, the Garnet Hill strand parallels the Banning strand. Currently, the distribution of dextral slip rates among the strands is not entirely clear and it is not clear how slip transfers across SGP to the San Bernardino strand to the Northwest. Recent work by *Blisniuk et al*. [2013] indicates a relatively high (~20 mm/year) slip rate on the Mission Creek strand Northwest of its junction with the Banning strand, although the geomorphic expression of this segment dwindles farther to the Northwest, and appears to be inactive within the San Bernardino mountains [*Kendrick et al.*, 2011]. Some slip from the Coachella strand is transferred onto the Banning strand, which has recent slip estimates of 4-5 mm/yr *Gold et al.* [[2015]. And *Gold et al.* [2015] raise the possibility of multiple faulting scenarios that may be consistent with current slip rate estimates, including 1) northwest propagating rupture that proceeds entirely on the Mission Creek segment but then is redirected on smaller faults toward the Eastern California Shear Zone, 2) rupture that is partitioned between the Banning and Garnet Hill strands, and 3) rupture that is distributed among all three main segments. The implications for each of these potential outcomes could be quite different in terms of their ability to propagate rupture through the SGP.

The recurrence interval of ruptures through the San Gorgonio Pass (500 – 1000 yr [*Yule and Heermance*, 2011]) is much longer than that of ruptures along the Coachella segment (100 – 200 yr [*Philibosian et al.*, 2011]) lending support to the inference that some northward ruptures do not make it through the SGP. In 2016, we undertook to perform dynamic models of potential earthquakes in the Eastern San Gorgonio Pass region to help assess likely rupture paths of earthquakes in this region. We used the most accurate fault representations available, as well as fault stresses determined through constant-traction and regional stress assumptions. We are also close to the implementation of stresses derived through long-term quasi-static modeling that is consistent with measured slip rates and uplift patterns in the region. The results will have important implications for earthquake occurrence in the SGP, as well as for seismic hazard throughout Southern California. This work dovetails very well with our own prior modeling efforts in the Western San Gorgonio Pass, as well as the broader work of the San Gorgonio Pass Special Fault Study Area (SFSA).

B. Methods

1. Estimating Fault Stress from Long-Term Modeling

The long-term modeling employs 3D Boundary Element Method (BEM) code, POLY3D. The 3D faults are discretized into triangles that are well suited for capturing the fault irregularities of the eastern San Gorgonio Pass region. To simulate deformation across the Southern SAF system, we apply plate boundary rates of displacement along the base of the model far from the investigated faults and allow the faults to slip freely and interact in response to this loading. The fault geometry for the quasi-static analysis follows the SCEC Community Fault Model v. 4 and contains over 30 active faults within and around the SGP. This approach follows that of successful models of the southern San Andreas fault system that closely match geologic slip rates and uplift patterns [e.g., *Fattaruso et al.*, 2014; *Herbert and Cooke*, 2012; *Herbert et al.*, 2014; *Marshall et al.*, 2009]. While we cannot know if the stress distributions produced by the models are correct, the correlation of model slip rates with geologic slip rates serves as a proxy for the error of the stress distributions.

The interseismic stressing-rates along the SAF can be simulated by applying slip-rates from the long-term multi-cycle model to each of the fault surfaces at depths below the base of seismicity (ie. locking depth). In this back-slip model, fault seismogenic zones are locked (above the base of seismicity) to simulate the accumulation of stresses during the interseismic period.

If we assume that each point on the fault surface follows a characteristic earthquake cycle with complete stress drop then the shear stress can be estimated from the time since last event and the shear stressing rate [e.g., *Smith-Konter and Sandwell*, 2009]. Because the stress rates vary along the fault due to complexities of fault interaction, the absolute stress can also vary greatly. Consequently, complex rupture behavior may emerge from these rather simple assumptions made for each element of the fault mesh.

The range of potential pre-rupture stress distributions is further expanded by considering the effects of earthquake events on nearby faults. Just as earthquakes appear to advanced the earthquake 'clock' on nearby faults [e.g., *Felzer et al.*, 2002; *Freed*, 2005; *King et al.*, 1994], earthquakes along nearby faults may produce stress distributions that impact the rupture dynamics along the San Andreas fault. To explore this effect, we simulate coseismic slip of recent ground-rupturing earthquakes recorded in sediments within [*Yule and Heermance*, 2011] and outside of the San Gorgonio Pass [e.g., *Biasi and Weldon*, 2009; *McGill et al.*, 2002; *Philibosian et al.*, 2011]. These events include: 1) the ~1680 event along the SAF in the Coachella Valley and within the SGP [*Philibosian et al.*, 2011] but not along the San Bernardino strand of the SAF [*Biasi and Weldon*, 2009], 2) the 1992 Landers earthquake [e.g., *Harris and Simpson*, 1992; *Parsons and Dreger*, 2000] and 3) the 1812 Wrightwood event along the San Bernardino strand [*Biasi et al*., 2009]. The resulting evolved tractions along the SAF thus include both the product of the long-term stressing rate and time since last rupture along the fault as well as the effects of these simulated earthquakes on nearby faults.

2. Dynamic Modeling

Our main dynamic modeling tool is the finite element code FaultMod [*Barall*, 2009]. This code has been validated by the SCEC/USGS dynamic earthquake rupture code verification exercise [*Harris et al.*, 2009] and can be used to model dynamic rupture on geometrically complex fault systems. In particular, we focus on the strand triplication area on the Eastern edge of San Gorgonio Pass. Our fault geometry (denoted the Cooke geometry is derived from that used in long-term quasi-static models of the region [*Fattaruso et al.,* 2014], but with finer discretization. The maximum depth allowed for rupture is set by the depth extent of local seismicity—approximately 20 km. For comparison, we also generate models using the SCEC Community Fault Model. We constructed our 3D meshes using TRELIS software (the successor to CUBIT); a low-resolution version of the Cooke mesh is shown in Figure 2. For simplicity we initially assume a homogeneous seismic velocity structure, but we may experiment with the SCEC Community Velocity Model in the future. We focus on earthquakes that nucleate on the Coachella Valley segment SW of the Banning/Mission Creek branch, because our main goal is to determine which branch(es) such earthquakes may take as they approach the SGP.

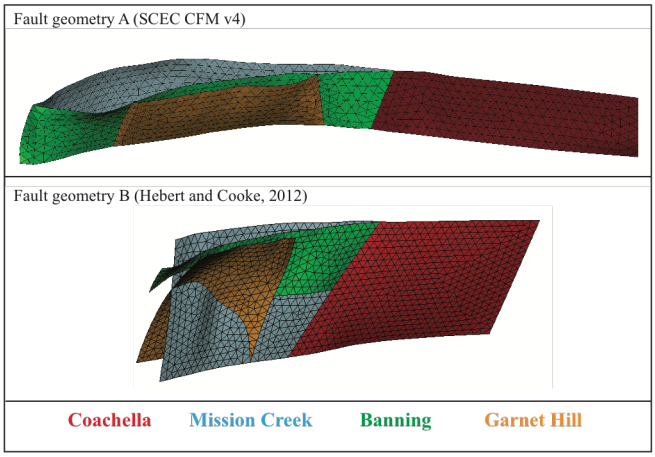

Figure 2. Fault geometries implemented in dynamic models based on long-term fault modeling. Models are based on different versions of the SCEC CFM.

C. Results

1. Estimating Fault Stress from Long-Term Modeling

The models explore the range of uncertainty of tectonic loading of the region. The relative motion between the North American and Pacific plates is estimated as 45-50 mm/yr at 320˚-325˚ from MORVEL [*DeMets et al.*, 2010] and GPS studies [*Argus et al.*, 2010; *Beavan et al.*, 2002; *Gonzalez-Garcia et al.*, 2003; *Kogan and Steblov*, 2008; *Marquez-Asua et al.*, 2004; *Plattner et al.*, 2007]. While 5˚ variations in plate velocity alter the distribution of slip rates along faults [*Herbert and Cooke*, 2012], the impact of these variations on interseismic stressing rates along the faults are small. Consequently, we report the results from an average of the tectonic loading range.

Considering time since last event. The evolved tractions are the produce of the interseismic stressing rate on the fault and the time since last event. The spatial variation in shear and normal stressing rate distributions reflects both the variations in long-term slip rates below the locking depth and fault interaction, both of which are greatly influenced by fault geometry (Fig. 3A). The distribution of stressing rates is 80% correlated with tractions resolved from remote stress tensor. However, these distributions do not consider the time since last event on each fault, which significantly alters the traction distribution (Fig. 3B & C) and reduces the correlation of resolved tractions

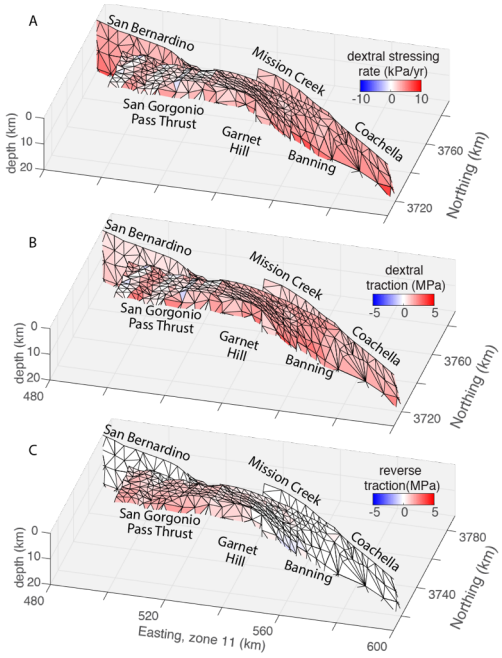

Figure 3: Distribution of evolved tractions along the San Andreas through the San Gorgonio Pass. Tractions are calculated using interseismic loading rates and time since last event on each segment.

from the remote stress tensor to 60%. While the time of last rupture cannot be confirmed on all fault segments, we used 1812 AD for last event along the San Bernardino strand [*Biasi et al.*, 2009], 1440 AD for last rupture on the San Gorgonio Pass thrust, Garnet Hill and Banning strands [*Yule and Heermance*, 2011], and 1680 AD for the last rupture on the Coachella and Mission Creek strands [*Philibosian et al.*, 2011]. Whereas dextral stressing rates are greater along the Coachella and Mission Creek strands, the Garnet Hill and Banning strands have greater evolved dextral traction due to their longer time since last event (Fig 3B).

Considering normal stress. Constraining absolute normal traction is more complex than for shear stress because we can't assume that normal tractions are relieved during rupture events. Consequently, the pattern of normal stressing rates over multiple earthquake cycles will guide normal traction distributions in the dynamic rupture models (Fig. 4). As expected, the normal stressing rates show increasing compressive stresses within the restraining bend of the SGP. This spatial variability in normal stressing rates suggests different degrees of clamping along the fault system, which will be applied to the dynamic rupture models.

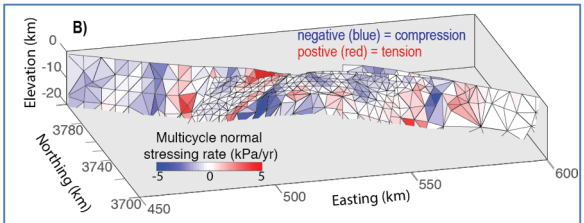

Figure 4: Normal stressing rate from the long-term quasi-static model shows variable clamping along faults. Regions of local tension develop within the restraining bend due to fault interaction.

Considering recent ruptures. Of the three earthquakes simulated, the 1812 earthquake has the greatest impact on shear tractions (Fig. 5). The Landers earthquake loads the SAF with < 0.5 MPa of right and left lateral shear along with some unclamping. The 1812 Wrightwood event loads the eastern San Gorgonio Pass Thrust with up to 1.5 MPa of dextral shear and the western portion of this fault with equal sinistral shear (Fig. 5). The 1680 earthquake loads the Banning and Garnet Hill strands with 1 MPa of dextral shear.

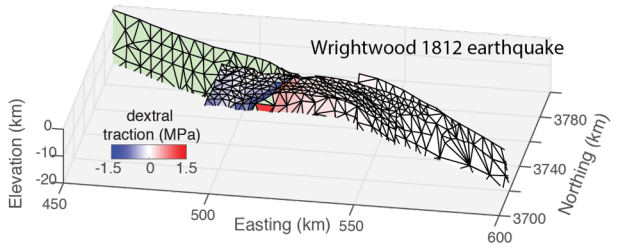

Figure 5. The 1812 earthquake is simulated with slip along the San Bernardino strand. Within the SGP, the shear tractions are impacted as much as 1.5 MPa near the southern end of the simulated rupture.

This work served as 1 chapter of a MS thesis at UMass – Amherst and also another UMass PhD student has contributed to this study.

2. Dynamic Modeling

Constant Traction Models: Our initial results, carried out by UCR Postdoc Roby Douilly, utilize a constant-traction stress model, with each fault surface element having the same initial normal and shear tractions. We test two different stress regimes, as shown in Figure 6. In the high-normal-stress case (top panel), both the SCEC CFM v. 4 geometry (left) and CFM v. 3 geometry (right) lead to rupture that proceeds only on the Mission Creek segment after the junction. In the low-normal-stress case (bottom panel), the rupture is able to propagate briefly to the Banning Strand in the CFM v. 4 geometry (left), after which it propagates to the Garnet Hill, dying out on the Banning. In contrast, the CFM v. 3 geometry (right) does not seem to support rupture to the Banning or Garnet Hill segments in either stress regime.

Regional Stress Models: As a potentially more realistic set of stress inputs, we use a regional stress field based on the work of *Hardebeck and Hauksson* [2001], with a principle stress azimuth 10° East of North. This constant stress tensor is resolved into different shear and normal stress values on each fault element due to its orientation. We find a significant component of dip-slip stress in many locations including on the Mission Creek and Banning strands. On the CFM v. 4 geometry, rupture propagates to all strands except for the Garnet Hill, while on the CFM v. 3 geometry, rupture propagates to all fault strands. We note that propagation to all strands in the CFM v. 3 geometry may be related to the greater connectivity between the Garnet Hill and other strands compared to the v. 4 geometry.

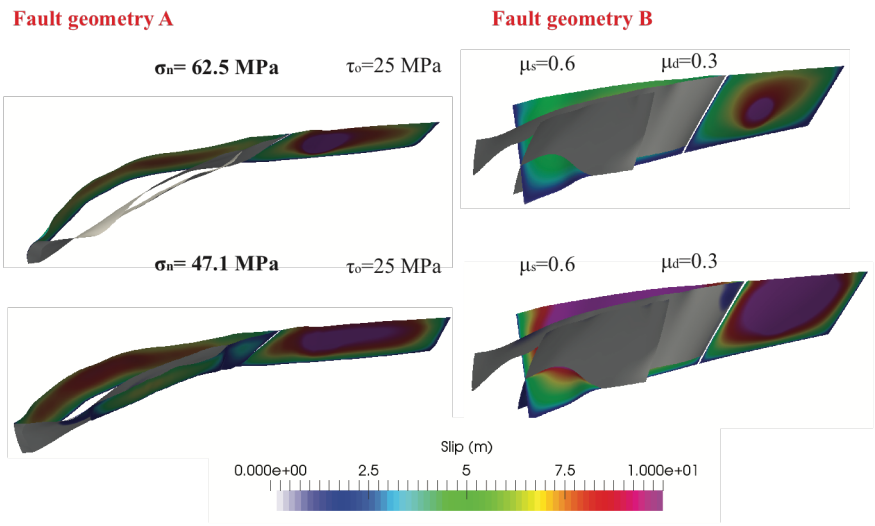

Figure 6. Dynamic modeling results for constant traction cases. High-normal-stress models are on top, and low-normal-stress models are on bottom; SCEC CFM v. 4 fault geometry is on left, and CFM v3 fault geometry is on right. The results differ for different stress assumptions and different geometries.

Preliminary Discussion: The current results indicate that the rupture path for potential earthquakes in the Eastern San Gorgonio Pass may depend strongly on both the assumed fault geometry as well as the assumed stress pattern. Indeed, it is remarkable that two different fault geometries that fit observations roughly equally can produce such different results. Nonetheless, it appears that under some reasonable assumptions about stress, the Mission Creek appears to be more favorable for rupture propagation than the more southerly strands. The dynamic results clearly call for a more realistic, physically-motivated set of stresses, which will be provided by the long-term modeling. Our progress in this area is poising us very well to continue this research in the upcoming year. In particular, by using the evolved stresses both on- and off-fault, we will be situated to include off-fault failure in future modeling efforts.

Our results may have important implications for seismic hazard in both the immediate San Gorgonio Pass region and wider Southern California. The current results imply that the northern route toward the San Gorgonio Pass may be more favorable for rupture than the southern routes that appear to connect through the San Gorgonio Pass thrust fault system. Thus, it may be very important to determine the degree of fault activity and connectivity for the northern strands, such as the Mission Creek and Mill Creek. This kind of work is a hot topic for the continued work of the SCEC community as part of the San Gorgonio Pass SFSA and beyond into SCEC5.

References

Argus, D., R. Gordon, M. Heflin, C. Ma, R. Eanes, P. Willis, W. R. Peltier, and S. Owen (2010), The angular velocities of the plates and the velocity of Earth's center from space geodesy, *Geophysical Journal International*, *180*, 913-960.

Barall, M. (2009), A grid-doubling technique for calculating dynamic three-dimensional spontaneous rupture on an earthquake fault, *Geophysical Journal International*, *178*, 845-859.

Beavan, J., M. Tregoning, M. Bevis, T. Kato, and C. Meertens (2002), Motion and rigidity of the Pacific plate and implications for plate boundary deformation, *Journal of Geophysical Research*, *107*(B10), 1-15.

Biasi, G., and R. Weldon (2009), San Andreas Fault Rupture Scenarios from Multiple Paleoseismic Records: Stringing Pearls, *Bulletin of the Seismological Society of America*, *99*, 471-498, doi:10.1785/0120080287.

Blisniuk, K., K. M. Scharer, W. D. Sharp, R. Burgmann, M. J. Rymer, and P. L. Williams (2013), New slip rate estimates for the Mission Creek strand of the San Andreas fault zone, paper presented at AGU Fall Meeting, American Geophysical Union, San Francisco, CA.

DeMets, C., R. G. Gordon, and D. F. Argus (2010), Geologically current plate motions, *Geophysical Journal International*, *181*, 1-80.

Fattaruso, L. A., M. L. Cooke, and R. J. Dorsey (2014), Sensitivity of uplift patterns to dip of the San Andreas fault in the Coachella Valley, California, *Geosphere*, *10*(6), 1235-1246, doi:10.1130/GES01050.1.

Felzer, K. R., T. W. Becker, R. E. Abercrombie, G. Ekström, and J. R. Rice (2002), Triggering of the 1999 MW 7.1 Hector Mine earthquake by aftershocks of the 1992 MW 7.3 Landers earthquake, *Journal of Geophysical Research*, *107*, doi:10.1029/2001JB000911.

Freed, A. (2005), Earthquake triggering by static, dynamic and postseismc stress tranfser, *Annual Review of Earth and Planetary Science*, 335-367, doi:10.1146/annurev.earth.33.092203.122505.

Gold, P. O., W. M. Behr, D. H. Rood, W. D. Sharp, T. Rockwell, K. J. Kendrick, and A. Salin (2015), Holocene geologic slip rate for the Banning strand of the southern San Andreas Fault, southern California, *Journal of Geophysical Research*, *120*, 5639-5663, doi:10.1002/ 2015JB012004.

Gonzalez-Garcia, J. J., L. Prawirodirdjo, Y. Bock, and D. Agnew (2003), Guadalupe Island, Mexico as a new constraint for Pacific plate motion, *Geophysical Research Letters*, *30*(1872), doi:10.1029/2003GL017732.

Hardebeck, J. L., and E. Hauksson (2001), Crustal stress field in southern California and its implications for fault mechanics, *Journal of Geophysical Research*, *106*(B10), 21859-21882.

Harris, R. A., M. Barall, R. J. Archuleta, E. M. Dunham, B. Aagaard, J.-P. Ampuero, H. S. Bhat, V. Cruz-Atienza, L. Dalguer, P. Dawson, S. M. Day, B. Duan, G. Ely, Y. Kaneko, Y. Kase, N. Lapusta, Y. Liu, S. Ma, D. D. Oglesby, K. B. Olsen, A. Pitarka, S. G. Song, and E. Templeton (2009), The SCEC/USGS dynamic earthquake rupture code verification exercise, *Seismological Research Letters*, *80*(1), 119-126.

Harris, R. A., and R. W. Simpson (1992), Changes in static stress on southern California faults after the 1992 Landers earthquake, *Nature*, *360*, 251-254, doi:10.1038/360251a0.

Heermance, R. V., D. Yule, and I. Desjarlais (2015), Evidence for trans-San Gorgonio Pass earthquakes based on Holocene slip rates along the San Andreas Fault System at Millard Canyon, paper presented at Southern California Earthquake Center Annual Meeting, Palm Springs, CA.

Herbert, J. W., and M. L. Cooke (2012), Sensitivity of the southern San Andreas fault system to tectonic boundary conditions, *Bulletin of the Seismological Society of America*, *105*(2046-2062), doi:10.1785/0120110316.

Herbert, J. W., M. L. Cooke, and S. T. Marshall (2014), Influence of fault connectivity on slip rates in southern California: Potential impact on discrepancies between geodetic derived and geologic slip rates, *Journal of Geophysical Research*, *119*, 2342-2361, doi:10.1002/ 2013JB010472.

Kendrick, K. J., J. C. Matti, S. A. Mahan, G. P. Landis, and D. P. Miggins (2011), Depositional constraints on slip along the San Andreas fault within the eastern San Gorgonio Pass region, Southern California, *2011 SCEC Annual Meeting Program*, A-135.

King, G. C. P., R. S. Stein, and J. Lin (1994), Static stress chnges and the triggering of earthquakes, *Bulletin of the Seismological Society of America*, *84*, 935-953.

Kogan, M. G., and G. M. Steblov (2008), Current global plate kinematics from GPS (1995–2007) with the plate-consistent reference frame, *Journal of Geophysical Research*, *113*(B04416), doi:10.1029/2007JB005353.

Marquez-Asua, B., E. Cabral-Cano, F. Correa-Mora, and C. DeMets (2004), A model for Mexican neotectonics based on nationwide GPS measurements, *Geofisica Internacional*, *43*, 319-330.

Marshall, S. T., M. L. Cooke, and S. E. Owen (2009), Interseismic Deformation Associated with Three-Dimensional Faults in the Greater Los Angeles Region, California, *Journal of Geophysical Research*, *114*(B12403), doi:10.1029/2009JB006439.

McGill, S. F., S. A. Dergham, K. Barton, T. Berney-Ficklin, D. Grant, C. Hartling, K. Hobart, R. Minnich, M. Rodriguez, E. Runnerstrom, J. Russel, K. Schmoker, M. Stumfall, J. Townsend, and J. Williams (2002), Paleoseismology of the San Andreas fault at Plunge Creek near San Bernardino, southern California, *Bulletin of the Seismological Society of America*, *92*, 2803-2840.

Olsen, K. B., S. M. Day, J. B. Minster, Y. Cui, A. Chourasia, D. Okaya, P. Maechling, and T. Jordan (2008), TeraShake2: Spontaneous rupture simulations of M-w 7.7 earthquakes on the southern San Andreas fault, *Bulletin of the Seismological Society of America*, *98*(3), 1162-1185.

Parsons, T., and D. S. Dreger (2000), Static ‐ stress impact of the 1992 Landers earthquake sequence on nucleation and slip at the site of the 1999 M= 7.1 Hector Mine earthquake, southern California, *Geophysical Research Letters*, *27*, 1949-1952.

Philibosian, B., T. Fumal, and R. Weldon (2011), San Andreas Fault earthquake chronology and Lake Cahuilla history at Coachella, California, *Bulletin of the Seismological Society of America*, *101*(1), 13-38, doi:10.1785/0120100050.

Plattner, C., R. Malservisi, T. H. Dixon, P. LaFemina, G. Sella, J. Fletcher, and F. Suarez-Vidal (2007), New constraints on relative motion between the Pacific plate and Baja California microplate (Mexico) from GPS measurements, *Geophysical Journal International*, *170*, 1373-1380.

Smith-Konter, B., and D. Sandwell (2009), Stress evolution of the San Andreas fault system: Recurrence intervalversus locking depth, *Geophysical Research Letters*, *36*(L13304), doi:10.1029/2009GL037235.

Yule, D. (2009), The enigmatic San Gorgonio Pass, *Geology*, *37*(2), 191-192.

Yule, D., and R. Heermance (2011), Earthquake record and slip rate of the San Gorgonio Pass fault zone: Testing the ShakeOut scenario earthquake, *Southern California Earthquake Center Annual Report*.